

Quantum Noise, Scaling and Domain Formation in a Spinor BEC

George I. Mias,^{1,*} Nigel R. Cooper,^{2,†} and S. M. Girvin^{1,‡}

¹*Sloane Physics Laboratory, Yale University, New Haven, CT 06520-8120, USA*

²*T.C.M. Group, Cavendish Laboratory, J. J. Thomson Ave., Cambridge, CB3 0HE, UK*

(Dated: October 29, 2018)

In this paper we discuss Bose-Einstein spinor condensates for $F=1$ atoms in the context of ^{87}Rb , as studied experimentally by the Stamper-Kurn¹ group. The dynamical quantum fluctuations of a sample that starts as a condensate of N atoms in a pure $F = 1$, $m_F = 0$ state are described in analogy to the ‘two-mode squeezing’ of quantum optics in terms of an $\mathfrak{su}(1,1)$ algebra. In this system the initial $m_F = 0$ condensate acts as a source (‘pump’) for the creation pairs of $m_F = 1, -1$ atoms. We show that even though the system as a whole is described by a pure state with zero entropy, the reduced density matrix for the $m_F = +1$ degree of freedom, obtained by tracing out the $m_F = -1, 0$ degrees of freedom, corresponds to a thermal state. Furthermore, these quantum fluctuations of the initial dynamics of the system provide the seeds for the formation of domains of ferromagnetically aligned spins.

PACS numbers: 03.75.Mn, 03.75.Lm, 03.75.Kk

I. INTRODUCTION

Spinor condensates were first realized^{2,3} in 1998. Such condensates are very rich in the underlying physics and have been the subject of numerous studies, from mean field theory and ground state considerations^{4,5,6} to experimental observation of dynamics, rotation effects, domain structures^{7,8,9,10,11,12}, theoretical dynamics of mixing^{13,14,15}; existence of quantum vortices and topological structure^{16,17,18,19}; dipolar effects²⁰ and very many more, currently making this one of the most active fields at the interface between condensed matter and atomic physics.

In this paper we investigate the formation of domains in terms of a Bose-Einstein spinor condensate of alkali atoms, ^{87}Rb , in the hyperfine multiplet $F = 1$, which has been shown to have ferromagnetic interaction amongst the constituent atoms^{4,6,9}. A recent experiment carried out by the Stamper-Kurn group at Berkeley¹, showed the formation of domains in a ^{87}Rb gas starting with a polar non-ferromagnetic initial state. The experimental sample formed random domains of varying transverse magnetization, and this paper is based on considerations regarding this experiment and the dynamical seeding of the observed domains. The analysis of this experiment has been undertaken by Lamcraft¹² who derived a form for the dynamics of the particles in different states. The dynamics of the associated quantum phase transition and scaling properties of the system magnetization has been discussed by Damski et al.²¹ for a one-dimensional system treated in a mean-field approach, with extensions to higher dimensions. The recent work of Saito et al.²² further investigated the dynamic formation of these domains in terms of quantum noise, including a simulation of two-dimensional domains using a combination of quantum dynamics and Gross-Pitaevskii evolution - this work was completed concurrently with our own investigation with essentially the same conclusions²³. In this paper we discuss an alternate, yet equivalent description of the

experimental work, which elucidates the nature of the quantum statistics. After introducing the system and the relevant experiment in Secs. I-II, we proceed in Sec. III to supplement previous results on the single-mode problem by providing a connection to the ideas of quantum squeezing and quantum noise, as well as some exact solutions to the dynamical single-mode problem. In Sec. IV we also follow a multi-mode approach, in terms of which the time evolution, quantum noise and statistics of the domain seeding may be discussed. This is presented in connection to an $\mathfrak{su}(1,1)$ algebra inherent in the effective Hamiltonian derived for the system, making it possible to obtain probability distributions for the fluctuations in the system. As we will see the thermal nature of these distributions is distinctive and might be verifiable experimentally.

A. Effective theory of spinor condensates

The use of dipolar optical traps allows for Bose-Einstein condensation of alkali atoms in which the spin degree of freedom is still active - the traps do not preferentially select one of the spin states with a given m_F (as opposed to magnetic traps that favor the weak-field seeking states). Thus for a gas of spin F there are $2F + 1$ degrees of freedom deriving from the hyperfine spin. The total spin for both ^{87}Rb and ^{23}Na is the sum of the nuclear spin, $I = 3/2$, and the electronic spin $S = 1/2$, leading to a total spin $F = 3/2 \pm 1/2$. For the $F = 1$ manifold, which is usually probed in optical trap experiments, this means that the atoms may be described by a spinor,

$$\psi(\mathbf{r}) = \begin{pmatrix} \psi_1(\mathbf{r}) \\ \psi_0(\mathbf{r}) \\ \psi_{-1}(\mathbf{r}) \end{pmatrix}, \quad (1)$$

with each component, $\psi_i(\mathbf{r})$, corresponding to the wave function of a species in the $m_F = \{-1, 0, 1\}$ state. At

zero magnetic field the system's spin rotational invariance is manifest. The standard Hamiltonian for the low energy dynamics of an $F = 1$ dilute atomic gas was developed by Ho⁴ and Ohmi and Machida⁶. This assumes that only two-body collisions are important and that the atoms do not interact otherwise with each other and that the system is rotationally invariant, which means that the interactions can only depend on the total spin \mathcal{F} of the colliding atoms and not on \mathcal{F}_z ^{24,25,26,27}. The complete effective Hamiltonian for the $F = 1$ dilute cold gases in second quantized form is written as,

$$H = \int d^3\mathbf{r} \left\{ \psi_i^\dagger(\mathbf{r}) \left(-\frac{\hbar^2 \nabla^2}{2m} \right) \psi_i(\mathbf{r}) + \psi_i^\dagger(\mathbf{r}) V_{ij} \psi_j(\mathbf{r}) + \frac{1}{2} \left[c_0 \psi_i^\dagger(\mathbf{r}) \psi_j^\dagger(\mathbf{r}) \psi_i(\mathbf{r}) \psi_j(\mathbf{r}) + c_2 \left(\psi_i^\dagger(\mathbf{r}) \mathbf{F}_{ij} \psi_j(\mathbf{r}) \right) \cdot \left(\psi_k^\dagger(\mathbf{r}) \mathbf{F}_{kl} \psi_l(\mathbf{r}) \right) \right] \right\}, \quad (2)$$

where V_{ij} is the trapping potential, the indices refer to the hyperfine species, $i, j \in \{-1, 0, 1\}$, and we are using the Einstein summation convention of summing over repeated indices. $\mathbf{F} \equiv \{F_x, F_y, F_z\}$ is a vector of spin-one matrices. We have also identified the couplings

$$c_0 \equiv \frac{4\pi\hbar^2}{3m} (2a_2 + a_0), \quad (3)$$

$$c_2 \equiv \frac{4\pi\hbar^2}{3m} (a_2 - a_0), \quad (4)$$

which depend on only two parameters, the scattering lengths a_0 and a_2 . The field operators obey the commutation relations,

$$[\psi_i(\mathbf{r}), \psi_j^\dagger(\mathbf{r}')] = \delta_{i,j} \delta^3(\mathbf{r} - \mathbf{r}'), \quad (5)$$

with all other commutators being zero. The trapping potential, V_{ij} is the result of a combination of magnetic and optical potentials and may be taken as diagonal, $V(\mathbf{r})$,

assuming that all magnetic fields are in the 'z-direction'. We should keep in mind that in writing the Hamiltonian in terms of projecting onto total spin \mathcal{F} subspaces we are assuming that any Zeeman shifts are smaller than the hyperfine splitting so that \mathcal{F} is still a good quantum number. The mean field analysis of this Hamiltonian^{4,6,13,15} indicates that the ground state for $c_2 < 0$, as is the case for ⁸⁷Rb, is ferromagnetic,

$$\zeta_0 = \exp[i\theta] U(\beta_1, \beta_2, \beta_3) \begin{pmatrix} 1 \\ 0 \\ 0 \end{pmatrix} = \exp[i\theta - \beta_3] \begin{pmatrix} \exp[-i\beta_1] \cos\left[\frac{\beta_2}{2}\right]^2 \\ \sqrt{2} \cos\left[\frac{\beta_2}{2}\right] \sin\left[\frac{\beta_2}{2}\right] \\ \exp[i\beta_1] \sin\left[\frac{\beta_2}{2}\right]^2 \end{pmatrix}, \quad (6)$$

which is written this way to emphasize that we have a degenerate set of ground states which are related to each other by a gauge transformation, $\exp[i\theta]$, and an arbitrary rotation via

$$U(\beta_1, \beta_2, \beta_3) \equiv \exp[-iF_z\beta_1] \exp[-iF_y\beta_2] \exp[-iF_z\beta_3], \quad (7)$$

where $\{\beta_1, \beta_2, \beta_3\}$ are the Euler angles²⁸. The application of a magnetic field would lead to the average spin pointing in the direction of the applied field and the selection of one of the degenerate ground states. In the absence of a field we have spontaneous symmetry breaking, where the system selects at random one of the possible directions for its spins.

We may write the field operators for the case of a homogeneous system as a plane wave expansion:

$$\psi_i(\mathbf{r}) = \frac{1}{\sqrt{V}} \sum_{\mathbf{k}} a_{i\mathbf{k}} \exp[i\mathbf{k} \cdot \mathbf{r}]. \quad (8)$$

This gives:

$$H_I = \frac{1}{2V} \sum_{\mathbf{k}_1 + \mathbf{k}_2 = \mathbf{k}_3 + \mathbf{k}_4} \left\{ (c_0 + c_2) (a_{1\mathbf{k}_1}^\dagger a_{1\mathbf{k}_2}^\dagger a_{1\mathbf{k}_3} a_{1\mathbf{k}_4} + a_{-1\mathbf{k}_1}^\dagger a_{-1\mathbf{k}_2}^\dagger a_{-1\mathbf{k}_3} a_{-1\mathbf{k}_4}) + c_0 a_{0\mathbf{k}_1}^\dagger a_{0\mathbf{k}_2}^\dagger a_{0\mathbf{k}_3} a_{0\mathbf{k}_4} + 2(c_0 + c_2) (a_{1\mathbf{k}_1}^\dagger a_{0\mathbf{k}_2}^\dagger a_{1\mathbf{k}_3} a_{0\mathbf{k}_4} + a_{-1\mathbf{k}_1}^\dagger a_{0\mathbf{k}_2}^\dagger a_{-1\mathbf{k}_3} a_{0\mathbf{k}_4}) + 2(c_0 - c_2) a_{1\mathbf{k}_1}^\dagger a_{-1\mathbf{k}_2}^\dagger a_{1\mathbf{k}_3} a_{-1\mathbf{k}_4} + 2c_2 (a_{1\mathbf{k}_1}^\dagger a_{-1\mathbf{k}_2}^\dagger a_{0\mathbf{k}_3} a_{0\mathbf{k}_4} + a_{0\mathbf{k}_1}^\dagger a_{0\mathbf{k}_2}^\dagger a_{1\mathbf{k}_3} a_{-1\mathbf{k}_4}) \right\}. \quad (9)$$

The interaction involves self-scattering and cross-scattering terms among the three particle flavors, in addition to the last term which involves the conversion of pairs of $m_F = 0$ particles to $m_F = \pm 1$ and vice versa. This provides for interesting interspecies dynamics that we will explore further in later sections.

II. AN INTERESTING EXPERIMENT ON ⁸⁷Rb

In an interesting experiment carried out by the Stamper-Kurn group at Berkeley¹, an initial sample of ⁸⁷Rb atoms was prepared in the $m_F = -1$ state and

trapped in a quasi-two-dimensional optical trap with oscillation frequencies $\{\omega_x, \omega_y, \omega_z\} = 2\pi\{56, 350, 4.3\}\text{s}^{-1}$ at a longitudinal magnetic field $B_z = 2\text{G}$. Subsequently, the atoms were converted to the $m_F = 0$ state by the application of a radio frequency(r.f.) field, reaching a peak density of $n = 2.8 \times 10^{14}\text{cm}^{-3}$. The magnetic field was then quickly ramped down linearly in 5ms to about 50mG and the gas was allowed to evolve freely in the trap. The presence of the original magnetic field provides a quadratic Zeeman interaction which lifts the degeneracy for the transitions $|m_F = -1\rangle \rightarrow |m_F = 0\rangle$ and $|m_F = 0\rangle \rightarrow |m_F = 1\rangle$ states, so that good conversion may be achieved from the initial $m_F = -1$ states to $m_F = 0$ states. Since $c_2 < 0$ for ^{87}Rb , the interactions are ferromagnetic in nature, and it is thus energetically favorable for the spins to align with each other. So, when the magnetic field is ramped down and becomes effectively zero, the $m_F = 0$ states become dynamically unstable because of the exchange interaction and convert to $m_F = \pm 1$ pairs. The different variables in the experiment are summarized in Table(I). Within some time, T_{hold} , the transverse magnetization in the xy -plane was then imaged, using a novel non-destructive in situ technique, by detecting its Larmor precession about a guide field. The experiment revealed that the longitudinal magnetization was negligible. In contrast, the images of the transverse magnetization, indicated the formation of multiple randomly oriented domains of varying shapes and sizes, as well as more involved spin textures. The typical size, ξ_{exp} , of the domains seen after the domain growth saturated was in the region of $\sim 10\mu\text{m}$. The growth of the transverse magnetization was observed to be initially exponential, with a time constant $\tau \sim 15(4)\text{ms}$.

If one tries to model the initial seeding of these domains using the Gross-Pitaevskii equations and starting from a pure $|N\rangle_{m_F=0}$ state, then no evolution of transverse magnetization is observed^{15,18}. We may think of the Gross-Pitaevskii equations as corresponding to non-linear Schrödinger equation describing the motion that begins sitting on top of a potential hill. Without an initial displacement nothing happens classically. Some form of noise is required to provide the instability to roll off down the potential hill. In a recent paper by Saito et al.¹⁸ different forms of noise, such as white noise or noise due to the unconverted initial $m_F = -1$ population, were tried out to reproduce the instability seen in the experiment by Sadler et al.¹. In this paper we instead model the instability that causes the seeding of the domains observed experimentally in terms of quantum noise, and obtain an analytic form for this in the initial time regimes that the seeding takes place. Recent work by Saito et al.²² uses a similar picture.

^{87}Rb data	
a_0 scattering length	101.8 a_B
a_2 scattering length	100.4 a_B
Mass	87 g mol ⁻¹
Experimental Parameters	
Number of atoms	$2.1(1) \times 10^6$
Peak density, n	2.8×10^{14} cm ⁻³
Temperature, T	40 nK
$c_0 n/k_B$ energy scale	~ 100 nK
$c_2 n/k_B$ energy scale	~ 480 pK
Trap frequencies $\{\omega_x, \omega_y, \omega_z\}$	$2\pi\{56, 350, 4.3\}$ s ⁻¹
Initial magnetic field, B_z	2 G
Final magnetic field, B_z	50 mG
Time duration, T_{hold}	36-216 ms
$\hbar/(c_2 n)$ time scale	~ 15.8 ms
Observed time constant, τ	15(4) ms
Typical domain size, ξ_{exp}	~ 10 μm

TABLE I: Experimental values of interest for an experiment on ^{87}Rb ¹.

III. THE SINGLE MODE HAMILTONIAN AND ITS DYNAMICS

The simplest approach one can take beyond mean-field theory is to look at the single mode Hamiltonian. This has been done by various authors^{13,29}, including some numerical work within a classical framework^{19,30,31}. In this section we will independently reproduce some of the previous results in a different approach and supplement them with new insights.

We start with the effective Hamiltonian, for N spin-1 bosons in zero magnetic field and we assume that all the m_F species have the same spatial wave function, $\eta(\mathbf{r})$. This wave function is determined by using a Gross Pitaevskii equation which comes from the kinetic part of the Hamiltonian and the c_0 coupling - the symmetric parts of the Hamiltonian, Eq.(2). Namely,

$$\left(-\frac{\hbar^2}{2m}\nabla^2 + V + c_0 N |\eta(\mathbf{r})|^2\right) \eta(\mathbf{r}) = \mu_0 \eta(\mathbf{r}), \quad (10)$$

where μ_0 is a chemical potential enforcing the total particle conservation. Since for ^{87}Rb $c_0 \gg c_2$, this means the spatial wave functions, $\eta(\mathbf{r})$, of the condensate are largely dependent on c_0 and may be taken to be the same for each m_F species to a first approximation. The fields are thus approximated by

$$\psi_i(\mathbf{r}) = \eta(\mathbf{r}) a_i; \quad \psi_i(\mathbf{r})^\dagger = \eta(\mathbf{r})^* a_i^\dagger. \quad (11)$$

Here we have defined the operators a_i, a_i^\dagger that respectively annihilate or create a boson in the state $F_z = m_F = i$, with $i \in \{-1, 0, 1\}$ in the z -basis representation of the spin-1 operators. These operators obey the commutation relation

$$[a_i, a_j^\dagger] = \delta_{i,j}, \quad (12)$$

with other commutators being zero. We can further define a number operator that counts the number of bosons

in the state i as $\hat{N}_i = a_i^\dagger a_i$. Using these operators, and taking into account the total number conservation, $N = \hat{N}_0 + \hat{N}_1 + \hat{N}_{-1}$, we may rewrite the Hamiltonian in the form of Diener et al.²⁹:

$$H_0 = \frac{c}{2} \left((\hat{N}_1 - \hat{N}_{-1})^2 + (2\hat{N}_0 - 1)(\hat{N}_1 + \hat{N}_{-1}) + 2a_1^\dagger a_{-1}^\dagger a_0^2 + 2a_1 a_{-1} (a_0^\dagger)^2 \right). \quad (13)$$

c is given by:

$$c = c_2 \int d^3r |\eta(r)|^4. \quad (14)$$

Notice here that the c_0 terms which would relate to density fluctuations vanish up to a constant and thus do not affect the dynamics of the system and do not enter the single-mode Hamiltonian considered above.

A. Dynamical considerations

We make here the Bogoliubov approximation that we may replace the annihilation-creation operators for the condensate with numbers, $a_0 \approx a_0^\dagger \approx \sqrt{N_0}$, up to a phase factor that we may neglect since we are later concerned only with expectation values where the phase would cancel out. This approximation is valid for extremely short times as if our initial state $|N\rangle_0$ condensate acts as an unlimited source for the creation of particles in the $m_F = \pm 1$ states that does not get depleted. Also, we notice that in this approximation, the numbers of particles in the two spin states $m_F = \pm 1$ are equal at all times. This means we can ignore the first term in Eq.(13) that involves the difference $(\hat{N}_1 - \hat{N}_{-1})$. Then the Bogoliubov approximation Hamiltonian becomes quadratic in the fields,

$$H_B = \frac{c}{2} \left((2N_0 - 1)(\hat{N}_1 + \hat{N}_{-1}) + 2N_0(a_1^\dagger a_{-1}^\dagger + a_1 a_{-1}) \right). \quad (15)$$

We may obtain Heisenberg equations of motion in this regime as follows:

$$i\hbar\partial_t a_1 = [a_1, H_0] = \frac{c}{2}(2N_0 - 1)a_1 + cN_0 a_{-1}^\dagger; \quad (16)$$

$$i\hbar\partial_t a_{-1}^\dagger = -\frac{c}{2}(2N_0 - 1)a_{-1}^\dagger - cN_0 a_1. \quad (17)$$

This system of linear differential equations can be solved exactly to give:

$$a_1(t) = A_1(t)a_1 + A_{-1}(t)a_{-1}^\dagger, \quad (18)$$

$$a_{-1}(t) = A_1^*(t)a_{-1}^\dagger + A_{-1}^*(t)a_1. \quad (19)$$

where operators with no explicit time dependence correspond to operators at initial times, $t = 0$, and in addition we have defined,

$$A_1(t) \equiv \cosh \left[\frac{ct\sqrt{4N_0 - 1}}{2\hbar} \right] - \frac{i(2N_0 - 1)}{\sqrt{4N_0 - 1}} \sinh \left[\frac{ct\sqrt{4N_0 - 1}}{2\hbar} \right], \quad (20)$$

$$A_{-1}(t) \equiv -\frac{2iN_0}{\sqrt{4N_0 - 1}} \sinh \left[\frac{ct\sqrt{4N_0 - 1}}{2\hbar} \right]. \quad (21)$$

B. Number averages and variances

It is interesting to calculate the expectation value of the operator $\hat{N}_1(t)$ starting with a ground state where $N_1 = 0$. From the results in the previous section and starting with the ground state $\langle 0 |_{m_F=-1} \langle N |_{m_F=0} \langle 0 |_{m_F=1} \equiv \langle 0; N; 0 |$ we get the number expectation values,

$$N_\mu(t) = \langle 0; N; 0 | \hat{N}_\mu(t) | 0; N; 0 \rangle = \left| \frac{2(N_0) \sinh \left[\frac{ct\sqrt{4N_0 - 1}}{2\hbar} \right]}{\sqrt{4N_0 - 1}} \right|^2, \quad (22)$$

with $\mu \in \{\pm 1\}$. This indicates rapid population transformation from N_0 to equal numbers of $m_F = \pm 1$ particles. The equality of m_F populations is guaranteed from the Hamiltonian and the conservation of the total number of particles and the total spin in the system. We may investigate the single-mode dynamics further by calculating the variance,

$$\sigma_\mu^2 = \overline{N_\mu(t)^2} - \left(\overline{N_\mu(t)} \right)^2 = |A_1|^2 |A_{-1}|^2 \quad (23)$$

$$= \frac{4 \sinh^2 \left[\frac{ct\sqrt{4N_0 - 1}}{2\hbar} \right] N_0^2 \left(4N_0 \left(N_0 \sinh^2 \left[\frac{ct\sqrt{4N_0 - 1}}{2\hbar} \right] + 1 \right) - 1 \right)}{(1 - 4N_0)^2} \quad (24)$$

$$= \overline{N_\mu(t)} \left(\overline{N_\mu(t)} + 1 \right). \quad (25)$$

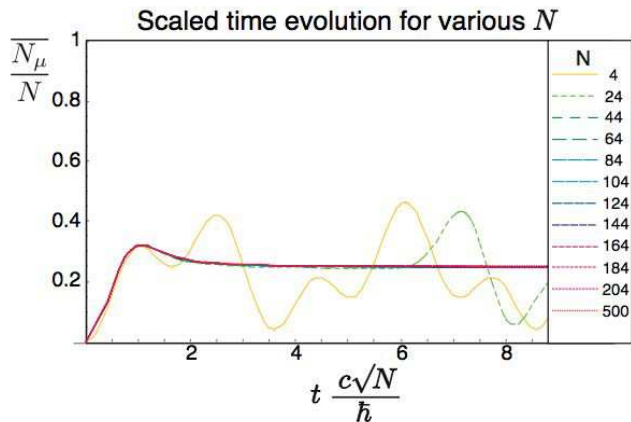


FIG. 1: (Color online) The single mode Hamiltonian may be solved exactly for different N . The time evolution of the solutions indicates scaling of $t \sim \frac{1}{\sqrt{N}}$ as the curves collapse into a single line for short times.

This is exactly the variance of a thermal state³² and it actually corresponds to a Bose-Einstein distribution - we will see this explicitly in the context of our multiple mode treatment in Sec.(IV C). The single mode condensate starts out with a source of N particles in the $m_F = 0$ pure state that are transmuted into equal numbers of $m_F = \pm 1$. Each of the resulting species displays a super-Poissonian variance, having a temperature and entropy associated with it. We should keep in mind that this is done in the Bogoliubov approximation and is in need of further exploration. Such considerations are undertaken in the next section for exact single mode solutions for various numbers of particles, as well as in Sec.(IV), which explores a multi-mode approximation.

C. Exact single mode solutions for different numbers of particles

We now turn our attention to solving the effective single mode Hamiltonian, Eq. (13) exactly for different initial numbers of particles N . Given our starting state $|N\rangle_{m_F=0}$, only pairs of particles may be created or destroyed, and this makes for a smaller subspace under our consideration. If we take our initial state to be the ‘number of pairs’ vacuum state, for N particles we may only have $\frac{N}{2} + 1$ number of pair-states. We may write the matrix components of the Hamiltonian that connects pair-states with i and j pairs respectively as:

$$\tilde{H}_{ij} \equiv \frac{c}{2} \left\{ 2i(2(N-2i)-1)\delta_{i,j} + 2\sqrt{(N-2j)(N-2j-1)}\delta_{i,j+1} + 2\sqrt{(N-2j+1)(N-2j+2)}\delta_{i,j-1} \right\}, \quad (26)$$

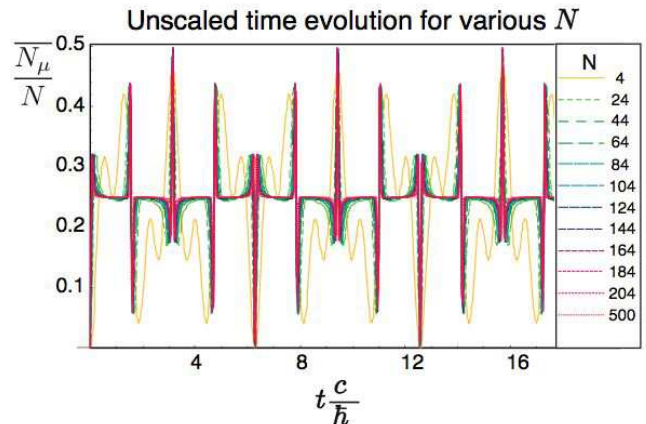


FIG. 2: (Color online) The exact solutions for the single mode Hamiltonian exhibit a linear time regime, with the curves for different N collapsing into a single curve without scaling. The populations oscillate and ultimately complete many cycles of non-linear evolution followed by linear evolution.

where $0 \leq i, j \leq N/2$. We may think of this as a hopping Hamiltonian, allowing for movement between adjacent states that differ by one pair. This is essentially a one-dimensional problem, resulting in a tridiagonal matrix that may be solved numerically to obtain the eigenvalues and time evolution of the system. The time evolution for various N is shown in the two figures, Fig.(1) and Fig.(2).

As we can see from the figures, we may identify a critical time $t_c \sim \frac{1}{\sqrt{N}}$ which separates two time regimes, in agreement with the results of Law et al¹³. We also notice the additional feature of scaling with $\frac{1}{\sqrt{N}}$ for short time scales, where the different evolutions for different total number of particles collapse into a single curve as

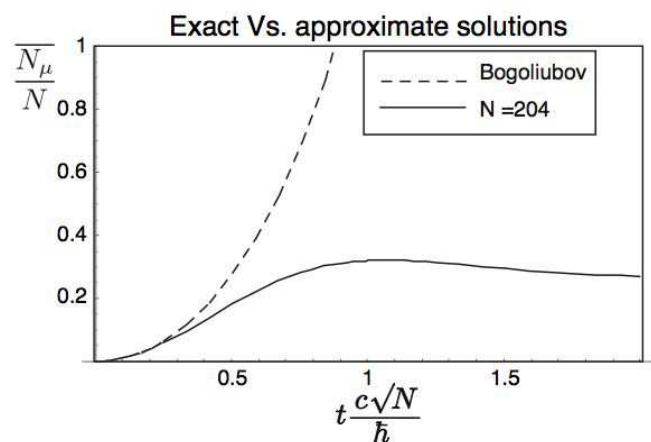


FIG. 3: The exact solution for $N = 204$ is compared to the Bogoliubov approximation. As is seen from the graph the two are in good agreement at the very early initial times, in support of our no-depletion approximation for the single mode Hamiltonian.

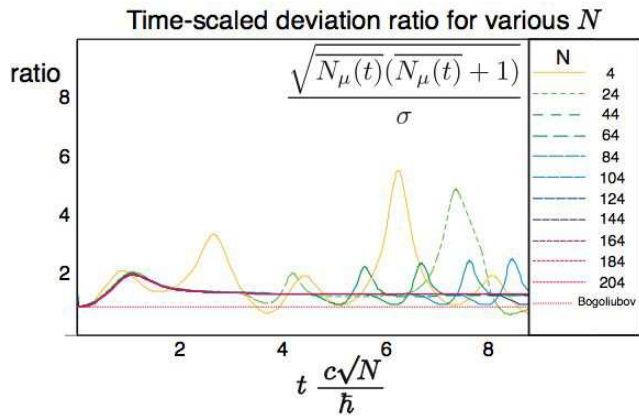


FIG. 4: (Color online) The ratio $\sqrt{N_\mu(t)(N_\mu(t) + 1)}$ to the deviation σ is a measure of the correlation of the state variance to that of a thermal state. Our Bogoliubov approximation is shown to obey a thermal variance and to match the exact results only for very short times. The various curves can be seen to collapse again into a single curve showing that the plotted ratio is independent of N .

seen in Fig.(1). There are two time regimes in the system: First a regime within which time scales as $\frac{1}{\sqrt{N}}$ when the dynamics is dominated by the non-linear part of the Hamiltonian shown in Fig.(1). Then we see a subsequent metastable time regime, when the linear part of the Hamiltonian takes over the time evolution and the time does not scale with the number of particles, Fig.(2). The time regimes alternate for many cycles if the system is allowed to evolve over time. The starting condensate of N particles in the $m_F = 0$ state is initially rapidly depleted to create pairs of $m_F = \pm 1$ particles. When the metastable time regime is reached, at $t \frac{c\sqrt{N}}{\hbar} = 1$, the population ratios are

$$\frac{N_{-1}}{N} : \frac{N_1}{N} : \frac{N_0}{N} \approx 0.25 : 0.25 : 0.5. \quad (27)$$

This metastable regime is followed by oscillations in the three different populations and eventually the complete repopulation of the $m_F = 0$ state, reaching again the initial state and the cycle repeating itself when $t \frac{c}{\hbar} = 2\pi$.

Furthermore, we may compare our Bogoliubov transformation for short times to the exact solution for a given N . As shown in Fig.(3) the two are in agreement only for very short times. Assuming the scaling of time with $\frac{1}{\sqrt{N}}$ this implies a validity time dictated by the depletion, where the percentage, κ_0 , of particles remaining in the $|N\rangle_{m_F=0}$ state is on the order of $\kappa_0 = \frac{N_0 - \sum_{\mu=\pm 1} -m_F=0 \langle N | \hat{N}_\mu | N \rangle_{m_F=0}}{N_0} \sim 0.9$. We are interested in the seeding of the domains at very early times in the time-evolution and hence the Bogoliubov approximation looks indeed like a good starting point.

Additionally, the statistical variance and deviation were investigated for various functional forms of the num-

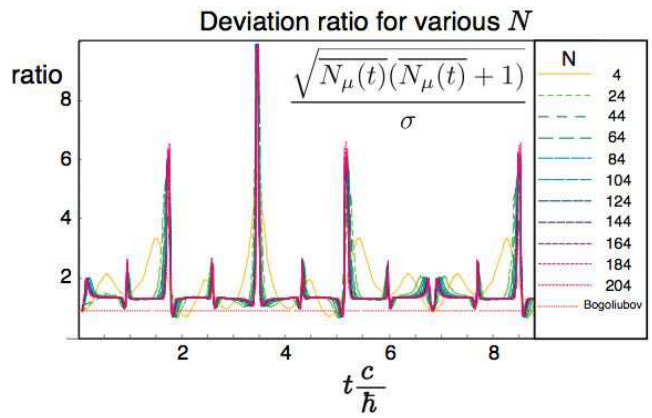


FIG. 5: (Color online) The ratio $\sqrt{N_\mu(t)(N_\mu(t) + 1)}$ to the deviation σ is here shown for long times. We still observe that our Bogoliubov approximation always obeys a thermal variance. Furthermore, the plot indicates that the plotted ratio is independent of N indicating that the actual variance is some functional of a thermal variance.

ber expectation, $\overline{N_\mu(t)}$. It was found that the curves for different number of particles collapse into single curves when we scale the variance with $\overline{N_\mu(t)(N_\mu(t) + 1)}$. Plots for different time scalings corresponding to the two time regimes identified above are shown in Fig.(4) and Fig.(5).

In the plots the ratio of $\sqrt{N_\mu(t)(N_\mu(t) + 1)}$ to the deviation σ , reveals scaling and collapse of the plotted curves showing that the deviation must be intimately related to a thermal distribution. The results of the Bogoliubov approximation are included for reference. As shown, the Bogoliubov approximation obeys a thermal variance through all time regimes, displaying super-Poissonian statistics consistent with two-mode squeezing picture^{33,34,35,36}, which will be discussed further in terms of the multimode approximation in the next section.

IV. MULTIMODE BOGOLIUBOV APPROXIMATION

We now would like to extend our discussion to the case of many spatial modes. The picture we have in mind is that $m_F = \pm 1$ pairs are created from the $m_F = 0$ source and then separate to begin seeding of the domains. The interplay of the various wavevectors \mathbf{k} will then be important in ascertaining the real space distribution and behavior of these domain seeds. We first look at an effective Hamiltonian description.

A. The effective multimode Hamiltonian

We begin with Eq.(9) and make the approximations that: we have no $m_F = 0$ atoms in a non-condensed state; self scattering and cross scattering terms outside

of the spinor $m_F = 0$ condensate maybe be ignored; we may take our Bogoliubov approximation once more for the $m_F = 0$ operators, $a_0 \sim a_0^\dagger \sim \sqrt{N}$. Then the effective Hamiltonian becomes,

$$H_{IB} = \frac{c_0}{2V}N^2 + N \sum_{\mathbf{k}} \left\{ \frac{(c_0 + c_2)}{V} (a_{1\mathbf{k}}^\dagger a_{1\mathbf{k}} + a_{-1\mathbf{k}}^\dagger a_{-1\mathbf{k}}) + \frac{c_2}{V} (a_{1\mathbf{k}}^\dagger a_{-1-\mathbf{k}}^\dagger + a_{1\mathbf{k}} a_{-1-\mathbf{k}}) \right\}. \quad (28)$$

As a simplification we will be assuming we can drop the c_0 terms in some short-time ‘no-depletion’ approximation since the variation of the c_0 terms with respect to N_0 approaches zero in this approximation - as we recall the terms cancel out identically in the single-mode approximation. The magnitude of the coupling ratio $\frac{c_0}{c_2} \sim 10^4$ suggests that density fluctuation modes, as dictated by the c_0 terms, are very stiff, so they are ignored in our calculations. We further neglect the spatial dependence of the trap potential. With all these simplifications made, we can finally write down the effective Hamiltonian we will use for our multimode treatment of the spinor condensate,

$$H_E = \sum_{\mathbf{k}} \left\{ (\epsilon_{\mathbf{k}} + c_2 n) (a_{1\mathbf{k}}^\dagger a_{1\mathbf{k}} + a_{-1\mathbf{k}}^\dagger a_{-1\mathbf{k}}) + c_2 n (a_{1\mathbf{k}}^\dagger a_{-1-\mathbf{k}}^\dagger + a_{1\mathbf{k}} a_{-1-\mathbf{k}}) \right\}, \quad (29)$$

where we have defined the kinetic energy,

$$\epsilon_{\mathbf{k}} \equiv \frac{\hbar \mathbf{k}^2}{2m}. \quad (30)$$

The effective Hamiltonian above treats the system in terms of pairs of the two species with $m_F = \pm 1$ having opposite wavevectors. The first term in the Hamiltonian counts the number of pairs and the second term provides an interaction via creation and annihilation of the said pairs. The Hamiltonian is quadratic in the field operators and thus we are looking fluctuations of the system at a gaussian level.

B. Time evolution of operators, noise and statistics

For a given mode we may obtain the following equations of motion,

$$\begin{aligned} i\hbar \frac{\partial a_{1\mathbf{k}}(t)}{\partial t} &= (\epsilon_{\mathbf{k}} + c_2 n) a_{1\mathbf{k}}(t) + c_2 n a_{-1-\mathbf{k}}^\dagger(t); \\ -i\hbar \frac{\partial a_{-1-\mathbf{k}}^\dagger(t)}{\partial t} &= (\epsilon_{\mathbf{k}} + c_2 n) a_{-1-\mathbf{k}}^\dagger(t) + c_2 n a_{1\mathbf{k}}(t). \end{aligned} \quad (31)$$

As for the single mode case these may be solved exactly to obtain

$$\begin{aligned} a_{1\mathbf{k}}(t) &= A_{1\mathbf{k}}(t) a_{1\mathbf{k}} + A_{-1-\mathbf{k}}(t) a_{-1-\mathbf{k}}^\dagger; \\ a_{-1-\mathbf{k}}^\dagger(t) &= A_{1\mathbf{k}}^*(t) a_{-1-\mathbf{k}}^\dagger + A_{-1-\mathbf{k}}^*(t) a_{1\mathbf{k}}, \end{aligned} \quad (32)$$

where we now have defined

$$\begin{aligned} A_{1\mathbf{k}}(t) &\equiv \cosh \left[\frac{t}{\hbar} G_{\mathbf{k}} \right] - \frac{i(c_2 n + \epsilon_{\mathbf{k}})}{G_{\mathbf{k}}} \sinh \left[\frac{t}{\hbar} G_{\mathbf{k}} \right]; \\ A_{-1\mathbf{k}}(t) &\equiv \frac{-i c_2 n}{G_{\mathbf{k}}} \sinh \left[\frac{t}{\hbar} G_{\mathbf{k}} \right], \end{aligned} \quad (33)$$

with an effective ‘gain’ function for a given mode \mathbf{k} ,

$$G_{\mathbf{k}}^2 \equiv \epsilon_{\mathbf{k}} (-2c_2 n - \epsilon_{\mathbf{k}}). \quad (34)$$

Again, in these solutions operators with no explicit time dependence refer to the initial time, $t = 0$, operators. The paper by Saito et al.²² also arrives at the same solutions to the differential equations, with a similar treatment of ignoring the c_0 terms. The current work supplements these with single mode considerations, and with an alternative treatment that is developed below: a quantum noise approach where a new connection is made to the $\mathfrak{su}(1, 1)$ language of quantum squeezing.

The two operators $a_{1\mathbf{k}}$, $a_{-1-\mathbf{k}}$ are closely intertwined, with the population of one acting as a noise source for the other and vice versa. This suggests also that the growth of different species with opposite wavevectors is a highly correlated process. Indeed, the correlation of species of opposite wavevectors is non-zero,

$$\begin{aligned} &{}_{m_F=0} \langle N | a_{-1\mathbf{k}'}(t) a_{1\mathbf{k}}(t) | N \rangle_{m_F=0} = \\ &= \left\{ \frac{c_2 n (c_2 n + \epsilon_{\mathbf{k}})}{G_{\mathbf{k}}} \sinh \left[\frac{t}{\hbar} G_{\mathbf{k}} \right]^2 - \frac{i c_2 n}{G_{\mathbf{k}}} \sinh \left[\frac{t}{\hbar} G_{\mathbf{k}} \right] \cosh \left[\frac{t}{\hbar} G_{\mathbf{k}} \right] \right\} \delta_{\mathbf{k}, -\mathbf{k}'}, \end{aligned} \quad (35)$$

where we may picture that the creation of a $|1\rangle_{1\mathbf{k}}$ state is correlated with the creation of a $|1\rangle_{-1-\mathbf{k}}$ state. The N -particle condensate source acts as a reservoir for the creation of pairs of particles moving in opposite directions. The $m_F = \pm 1$ states are populated rapidly, at an exponential rate, as shown by the evolution of the number expectation for a given wavevector:

$$\begin{aligned} \overline{N_{\mu\mathbf{k}}(t)} &= {}_{m_F=0} \langle N | \hat{N}_{\pm 1 \pm \mathbf{k}} | N \rangle_{m_F=0} \\ &= \frac{c_2^2 n^2}{G_{\mathbf{k}}^2} \sinh \left[\frac{t}{\hbar} G_{\mathbf{k}} \right]^2. \end{aligned} \quad (36)$$

We should note here that

$$\lim_{t \rightarrow 0} \overline{N_{\mu\mathbf{k}}(t)} = \frac{c_2^2 n^2 t^2}{\hbar^2}, \quad (37)$$

which agrees with our single mode considerations in the same limit, Eq.(22).

The exponential growth of the number of particles with time implies our no-depletion approximation is only valid in the initial stages of the time evolution. Furthermore, the growth is dominated by certain values of the magnitude of the wavevectors \mathbf{k} as seen by the behavior of $G_{\mathbf{k}}^2$,

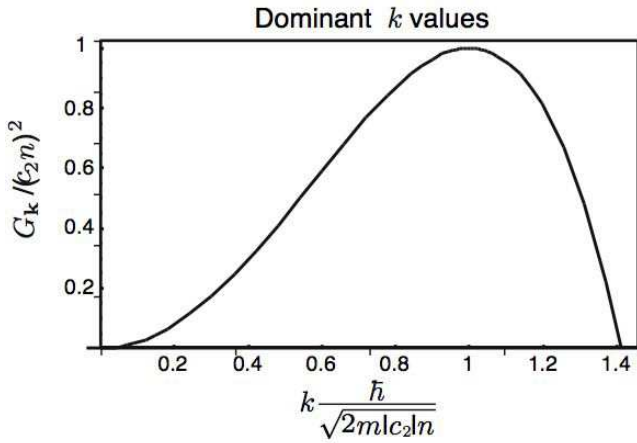


FIG. 6: The gain parameter $G_{\mathbf{k}}$ is real for only a set of values of k and these are the major contributors in the exponential growth of the number of $m_F = \pm 1$ particles. Imaginary values lead to oscillatory behavior instead which does not support the number growth of the two species.

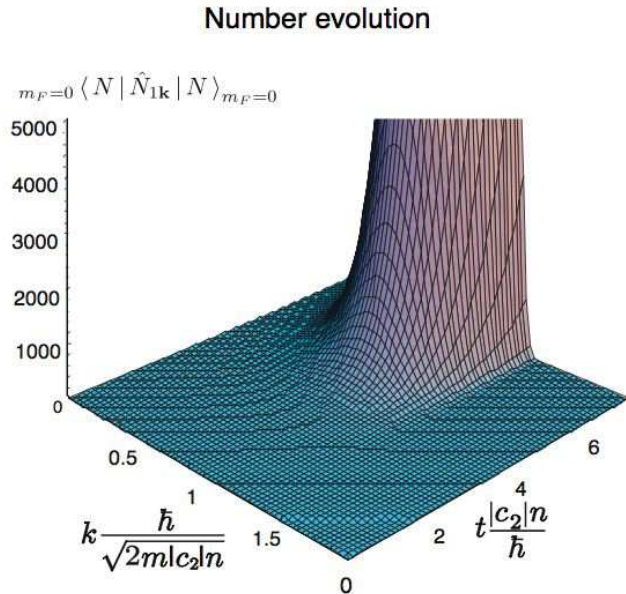


FIG. 7: (Color online) For ^{87}Rb , the expectation number of particles for a given species grows over a certain range of values of the wavevector magnitude k . Furthermore the growth in time is exponential and so our no-depletion approximation remains valid only at earlier times

Fig.(6), and is independent of direction. The dominant wavevector is at the maximum of $G_{\mathbf{k}}^2$:

$$k_{max} = \sqrt{\frac{-2mc_2 n}{\hbar^2}}. \quad (38)$$

This is the wave vector with the greatest initial instability. For ^{87}Rb , $c_2 < 0$ and hence $k_{max} \in \mathbf{R}$. It defines

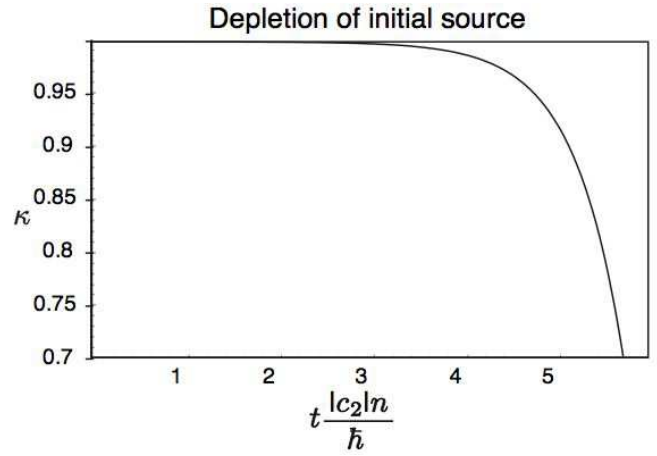


FIG. 8: The population of the $m_F = \pm 1$ species leads to the depletion of the initial source of N_0 atoms in the $m_F = 0$ state. Since our approximation assumes no depletion we can only ascertain its validity in the initial time region in the figure where it is only a few percent of the total available N_0 reservoir.

a coherence length scale,

$$\xi_0 \sim \frac{1}{k_{max}} = \sqrt{-\frac{\hbar^2}{2mc_2 n}} \approx 2.4 \mu\text{m}, \quad (39)$$

which in turn gives a coherence volume

$$V_{\xi_0} \sim \frac{4\pi \xi_0^3}{3}, \quad (40)$$

which for the experimental peak density, $n = 2.8 \times 10^{-14} \text{cm}^{-3}$, has associated with it $N_{\xi} = nV_{\xi_0} \sim 1.6 \times 10^4$ particles. This is large enough to support our assumption that the initial fluctuations are gaussian in nature, as suggested in our approximation of using a quadratic Hamiltonian. This allows us to explore the small quantum fluctuations that provide the starting instability for the evolution of the system - assuming no depletion of our initial particle source. We may investigate further by looking at the number evolution in time as a function of wavevector as shown in Fig. (7). This again shows the range of wavevectors over which the instability causes the growth of the $m_F = \pm 1$ states. Additionally, we observe that the growth is exponential in time, and that initially our depletion approximation should be valid. As an aside, we note here that for ^{23}Na $G_{\mathbf{k}}$ does not exhibit a real k_{max} since for this system $c_2 > 0$. Hence for ^{23}Na the number expectation values are oscillatory and no strong evolution into $m_F = \pm 1$ species would take place, consistent with the ‘antiferromagnetic’ interactions in this system³⁷. We may calculate the percentage of particles remaining in the $|N\rangle_{m_F=0}$ state source of the system as a function of time. We have,

$$\kappa = \frac{N_0 - \sum_{\mu, \mathbf{k}} \langle N | \hat{N}_{\mu \mathbf{k}} | N \rangle_{m_F=0}}{N_0}. \quad (41)$$

The sum may not be calculated in closed form, but may be approximated by integrating the wavevector over the “instability” range. The results are shown in Fig.(8), again indicating that at early times the depletion is only a few percent and our approximations must still be valid. For the characteristic time $t \frac{|c_2|n}{\hbar}$ we can substitute for the Berkeley experiment parameters to obtain each time unit as ~ 16 ms. Then up to say 4×16 ms in Fig.(8) corresponds to the first two initial images from the experiment, as shown in Fig.(2) in the paper by Sadler et al.¹. The experimental results are consistent with our no-depletion approximation for the initial times, when the domains are still forming and the transverse magnetization has not yet saturated as seen from the brightness of the figures.

1. Thermal Statistics

Having calculated the number expectation for a given species and mode it is natural to consider its variance. It turns out that we may express our result simply, in terms of the number operator expectation value in the $m_F = 0$ starting state evolving in time,

$$\begin{aligned} \sigma_{\mu\mathbf{k}}^2 &= \langle N_{\mu\mathbf{k}}(t)^2 \rangle - \langle N_{\mu\mathbf{k}}(t) \rangle^2 \\ &= \frac{c_2^2 n^2 (G_{\mathbf{k}}^2 + c_2^2 n^2 \sinh^2 [\frac{t}{\hbar} G_{\mathbf{k}}]) \sinh^2 [\frac{t}{\hbar} G_{\mathbf{k}}]}{G_{\mathbf{k}}^4} \\ &= \langle N_{\mu\mathbf{k}}(t) \rangle (\langle N_{\mu\mathbf{k}}(t) \rangle + 1). \end{aligned} \quad (42)$$

This is exactly the same form as for a thermal state. This may be slightly counterintuitive because we start out with a pure state at zero temperature, with no entropy associated with it and end up with essentially a thermal distribution (albeit with a different temperature for each spatial k mode). If we were to imagine that we were aware of the existence of only one of the two species, and carried a measurement of only that species for a given wavevector, we would associate a temperature to it based on its variance. Equivalently, we may think of this as what we would get if say we traced out the $m_F = -1$ atoms: the $m_F = 1$ atoms display an effective finite entropy and a thermal distribution. These super-Poissonian statistics show atom bunching and bear similarities to processes in as diverse fields as quantum optics^{33,34,35,38}, topological defects and particle production in cosmology and gravitation^{18,21,39,40,41,42,43}, within the common language of squeezing and the $\mathfrak{su}(1,1)$ algebra with which we

will recast our results in the following section. Furthermore, we will see how the thermal variance corresponds to a Bose-Einstein distribution using a reduced density matrix computation.

C. The $\mathfrak{su}(1,1)$ underlying algebra and evolution

We notice that our Hamiltonian H_E has an underlying structure in terms of pairs of different species and opposite wavevectors. Namely, we define operators that annihilate and create pairs at a given wavevector \mathbf{k} , $K_{\mathbf{k}}^-$ and $K_{\mathbf{k}}^+$ respectively, as well as an operator counting pairs, $K_{\mathbf{k}}^0$:

$$K_{\mathbf{k}}^- \equiv a_{1\mathbf{k}} a_{-1-\mathbf{k}}, \quad (43)$$

$$K_{\mathbf{k}}^+ \equiv a_{1\mathbf{k}}^\dagger a_{-1-\mathbf{k}}^\dagger, \quad (44)$$

$$K_{\mathbf{k}}^0 \equiv \frac{1}{2} (a_{1\mathbf{k}}^\dagger a_{1\mathbf{k}} + a_{-1-\mathbf{k}} a_{-1-\mathbf{k}}^\dagger). \quad (45)$$

The commutators of these operators turn out to be:

$$[K_{\mathbf{k}}^0, K_{\mathbf{k}}^\pm] = \pm K_{\mathbf{k}}^\pm, \quad (46)$$

$$[K_{\mathbf{k}}^+, K_{\mathbf{k}}^-] = -2K_{\mathbf{k}}^0, \quad (47)$$

providing a realization of the generators of an $\mathfrak{su}(1,1)$ algebra^{44,45}. In terms of these we may rewrite our effective Hamiltonian as,

$$H_E = \sum_{\mathbf{k}} \left\{ (\epsilon_{\mathbf{k}} + c_2 n) (2K_{\mathbf{k}}^0 - 1) + n c_2 (K_{\mathbf{k}}^+ + K_{\mathbf{k}}^-) \right\}. \quad (48)$$

We observe that the operators $K_{\mathbf{k}}^\pm$ create and annihilate pairs of atoms of different m_F species, with opposite wavevectors. Then $K_{\mathbf{k}}^0$ simply counts the number of these pairs in the system. We have thus arrived at the $\mathfrak{su}(1,1)$ algebra description that is associated with quantum squeezing. This is a multimode realization of the algebra, one realization per pair of atoms of different species and oppositely directed wavevectors. As we have already seen in the previous section the associated quantum states are characterized by thermal, super-Poissonian fluctuations, as was already discovered in our single-mode considerations.

Having obtained the form of the Hamiltonian we may now use it for unitary time evolution to arrive after time t to some final state $|f\rangle$,

$$|f\rangle = \exp \left[\frac{-i H_E t}{\hbar} \right] |N\rangle_{m_F=0} \quad (49)$$

$$= \prod_{\mathbf{k}} \exp[i\phi_{\mathbf{k}}] \exp \left[\frac{-it}{\hbar} \left\{ (\epsilon_{\mathbf{k}} + c_2 n) 2K_{\mathbf{k}}^0 + n c_2 (K_{\mathbf{k}}^+ + K_{\mathbf{k}}^-) \right\} \right] |N\rangle_{m_F=0}, \quad (50)$$

where,

$$\phi_{\mathbf{k}} \equiv \frac{t}{\hbar} (\epsilon_{\mathbf{k}} + c_2 n). \quad (51)$$

We want to disentangle the exponential as:

$$\exp[\theta \{a_{\mathbf{k}}^+ \hat{K}_{\mathbf{k}}^+ + a_{\mathbf{k}}^0 \hat{K}_{\mathbf{k}}^0 + a_{\mathbf{k}}^- \hat{K}_{\mathbf{k}}^-\}] = \exp[\phi_{\mathbf{k}}^+(\theta) \hat{K}_{\mathbf{k}}^+] \exp[\phi_{\mathbf{k}}^0(\theta) \hat{K}_{\mathbf{k}}^0] \exp[\phi_{\mathbf{k}}^-(\theta) \hat{K}_{\mathbf{k}}^-], \quad (52)$$

where θ is an auxiliary parameter which is set to one at the end and we have defined:

$$a_{\mathbf{k}}^+ = a_{\mathbf{k}}^- \equiv \frac{-it}{\hbar} n c_2, \quad (53)$$

$$a_{\mathbf{k}}^0 \equiv 2 \frac{-it}{\hbar} (\epsilon_{\mathbf{k}} + n c_2). \quad (54)$$

Matching the coefficients of the generators on both sides would give^{35,46}:

$$a_{\mathbf{k}}^+ = \dot{\phi}_{\mathbf{k}}^+ - \phi_{\mathbf{k}}^+ \dot{\phi}_{\mathbf{k}}^0 + (\phi_{\mathbf{k}}^+)^2 \dot{\phi}_{\mathbf{k}}^- \exp[-\phi_{\mathbf{k}}^0], \quad (55)$$

$$a_{\mathbf{k}}^0 = \dot{\phi}_{\mathbf{k}}^0 - 2\phi_{\mathbf{k}}^+ \dot{\phi}_{\mathbf{k}}^- \exp[-\phi_{\mathbf{k}}^0], \quad (56)$$

$$a_{\mathbf{k}}^- = \dot{\phi}_{\mathbf{k}}^- \exp[-\phi_{\mathbf{k}}^0]. \quad (57)$$

The last two equations may be substituted into the first to obtain a Riccati equation⁴⁷,

$$\dot{\phi}_{\mathbf{k}}^+ - (\phi_{\mathbf{k}}^+)^2 a_{\mathbf{k}}^- - \phi_{\mathbf{k}}^+ a_{\mathbf{k}}^0 - a_{\mathbf{k}}^+ = 0, \quad (58)$$

which gives the solutions:

$$\phi_{\mathbf{k}}^+(\theta) = \frac{a_{\mathbf{k}}^+}{\Gamma_{\mathbf{k}}} \frac{\sinh(\Gamma_{\mathbf{k}} \theta)}{\cosh(\Gamma_{\mathbf{k}} \theta) - \frac{a_{\mathbf{k}}^0 \sinh(\Gamma_{\mathbf{k}} \theta)}{2\Gamma_{\mathbf{k}}}}, \quad (59)$$

$$\phi_{\mathbf{k}}^0(\theta) = -2 \ln[\cosh(\Gamma_{\mathbf{k}} \theta) - \frac{a_{\mathbf{k}}^0 \sinh(\Gamma_{\mathbf{k}} \theta)}{2\Gamma_{\mathbf{k}}}], \quad (60)$$

$$\phi_{\mathbf{k}}^-(\theta) = \frac{a_{\mathbf{k}}^-}{\Gamma_{\mathbf{k}}} \frac{\sinh(\Gamma_{\mathbf{k}} \theta)}{\cosh(\Gamma_{\mathbf{k}} \theta) - \frac{a_{\mathbf{k}}^0 \sinh(\Gamma_{\mathbf{k}} \theta)}{2\Gamma_{\mathbf{k}}}}, \quad (61)$$

where

$$\Gamma_{\mathbf{k}}^2 = \frac{(a_{\mathbf{k}}^0)^2}{4} - a_{\mathbf{k}}^+ a_{\mathbf{k}}^- \quad (62)$$

$$= \frac{t^2}{\hbar^2} G_{\mathbf{k}}^2. \quad (63)$$

Our final state becomes:

$$|f(t)\rangle = \otimes_{\mathbf{k}} \left\{ \exp \left[\frac{\phi_{\mathbf{k}}^0}{2} + i\phi_{\mathbf{k}} \right] \sum_n (\phi_{\mathbf{k}}^+)^n |n\rangle_{1\mathbf{k}} |n\rangle_{-1-\mathbf{k}} \right\} \equiv \otimes_{\mathbf{k}} |f_{\mathbf{k}}(t)\rangle. \quad (64)$$

This is an exact solution for the dynamics of our effective Hamiltonian, H_E , in terms of number states for a given wavevector and particle species. We can either use the time-evolved state or simply the time-evolution of the creation annihilation operators to investigate the statistical behavior of the system and arrive at the familiar expression for two-mode squeezing

$$\langle N_{\mu\mathbf{k}}(t)^2 \rangle - \langle N_{\mu\mathbf{k}}(t) \rangle^2 = \langle N_{\mu\mathbf{k}}(t) \rangle (\langle N_{\mu\mathbf{k}}(t) \rangle + 1), \quad (65)$$

once again indicating that the variance for a given mode

is thermal in nature.

Let us investigate the thermal variance a bit further. Say we look at the density operator $\hat{\rho}_{\mathbf{k}}$ for a given wavevector, which for a pure state corresponds to

$$\hat{\rho}_{\mathbf{k}} = |f_{\mathbf{k}}(t)\rangle \langle f_{\mathbf{k}}(t)|. \quad (66)$$

We now perform a partial trace, to obtain the density matrix for the $m_F = 1$ particles after tracing out the $m_F = -1$ degrees of freedom for a given wavevector \mathbf{k} ,

$$\begin{aligned} \hat{\rho}_{+1\mathbf{k}} &= \text{Tr}_{m_F=-1} \hat{\rho}_{\mathbf{k}} \\ &= \frac{1}{\cosh \left[\frac{G_{\mathbf{k}} t}{\hbar} \right]^2 + \frac{(\epsilon_{\mathbf{k}} + n c_2)^2}{G_{\mathbf{k}}^2} \sinh \left[\frac{G_{\mathbf{k}} t}{\hbar} \right]^2} \sum_i \left(\frac{n^2 c_2^2 \sinh \left[\frac{G_{\mathbf{k}} t}{\hbar} \right]^2}{G_{\mathbf{k}}^2 \left(\cosh \left[\frac{G_{\mathbf{k}} t}{\hbar} \right]^2 + \frac{(\epsilon_{\mathbf{k}} + n c_2)^2}{G_{\mathbf{k}}^2} \sinh \left[\frac{G_{\mathbf{k}} t}{\hbar} \right]^2 \right)} \right)^i |i\rangle_{1\mathbf{k}} \langle i|_{1\mathbf{k}} \\ &= \frac{1}{1 + \overline{N_{1\mathbf{k}}(t)}} \sum_i \left(\frac{\overline{N_{1\mathbf{k}}(t)}}{1 + \overline{N_{1\mathbf{k}}(t)}} \right)^i |i\rangle_{1\mathbf{k}} \langle i|_{1\mathbf{k}}. \end{aligned} \quad (67)$$

An identical calculation but instead tracing out the $m_F = 1$ states gives,

$$\hat{\rho}_{-1\mathbf{k}} = \frac{1}{1 + \overline{N_{-1-\mathbf{k}}(t)}} \sum_i \left(\frac{\overline{N_{-1-\mathbf{k}}(t)}}{1 + \overline{N_{-1-\mathbf{k}}(t)}} \right)^i |i\rangle_{-1-\mathbf{k}} \langle i|_{-1-\mathbf{k}}. \quad (68)$$

The reduced density operators, $\hat{\rho}_{\pm 1\mathbf{k}}$, have exactly the form of the density matrix for a Bose-Einstein distribution^{38,48}. This is remarkable because our pair state $|f(t)\rangle$ is a pure state that has no entropy associated with it. On the other hand the reduced density operators, $\rho_{\pm 1\mathbf{k}}$, correspond to thermal Bose-Einstein distributions, that have an associated entropy and noise that results from the perfect correlations between the $m_F = \pm 1$ particles in each pair state. For a given wavevector, the $m_F = +1$ particles act as noise for the $m_F = -1$ particles and vice versa and hence production of pairs from our starting ‘vacuum’ provides a thermalization mechanism for a given particle species. The density operator depends on the wavevector \mathbf{k} indicating that the different modes of the system would receive different amounts of thermalization, and thus no single temperature may be associated to one or the other species for the entire

system. We may use the above results to produce simulations of the system similar to those of Saito et al.²². Saito et al. use the classical Gross-Pitaevskii equations but build in white noise to represent the quantum fluctuations. The white noise is chosen to reproduce the variance found in the fully quantum equations of motion which we use. Here we follow the the Q -function method of quantum optics. The Q -function of a density operator ρ is defined as³⁸

$$Q(\alpha, \alpha^*) \equiv \frac{1}{\pi} \langle \alpha | \rho | \alpha \rangle. \quad (69)$$

For a pure state this is proportional to the probability of the state to be in a coherent state α . For our representation of state $|f(t)\rangle$ we may write:

$$Q \equiv \frac{1}{\pi^{2\eta}} |\otimes_{\mathbf{k}} (\langle \alpha_{1\mathbf{k}} | \otimes \langle \alpha_{-1-\mathbf{k}} |) |f(t)\rangle|^2 \quad (70)$$

$$= \prod_{\mathbf{k}} \left(\frac{1}{\pi^2} \exp \left[\frac{\phi_{\mathbf{k}}^0 + \phi_{\mathbf{k}}^{0*}}{2} - |\alpha_{1\mathbf{k}}|^2 - |\alpha_{-1-\mathbf{k}}|^2 + \phi_{\mathbf{k}}^+ \alpha_{1\mathbf{k}}^* \alpha_{-1-\mathbf{k}}^* + \phi_{\mathbf{k}}^{+*} \alpha_{1\mathbf{k}} \alpha_{-1-\mathbf{k}} \right] \right) \quad (71)$$

$$\equiv \prod_{\mathbf{k}} Q_{\mathbf{k}}, \quad (72)$$

where η is the number of modes and we have used the expansion of coherent states in terms of number states,

$$|\alpha\rangle = \exp \left[-\frac{|\alpha|^2}{2} \right] \sum_l \frac{\alpha^l}{\sqrt{l!}} |l\rangle. \quad (73)$$

Given this probability distribution we notice that each $Q_{\mathbf{k}}$ is an exponential of a quadratic form and is thus gaussian in nature. A change of basis to diagonal form allows us to calculate the variance and select a random distribution of coherent state amplitudes consistent with this probability distribution. The random realizations thus obtained support our picture of quantum noise providing the seeds for the formation of domains, and reproduce the results of Saito et al.²².

The thermal nature of the fluctuations may be verifiable experimentally. An experiment could be undertaken that considers two settings: (i) a system with a starting state of N particles that have Bose-condensed in a ground

state of the system, say with $m_{F_z} = 1$ (any uniform rotation of such a state would do, since we are selecting one of the degenerate set of ground states for the system). For such an initial state, usually approximated as a coherent state, the number variance (or a corresponding density-density correlator^{34,49,50}) for the particles in the $m_{F_z} = +1$ (or -1) state is Poissonian in nature, i.e. $\sigma_{\mu\mathbf{k}=\mathbf{0}} \sim N$. The density-density correlator for non-zero wavevector \mathbf{q} , is calculated for particles in the $F_z = 1$ state and corresponds to having Poissonian shot noise:

$$\begin{aligned} C_{+\mathbf{q}} &\equiv {}_{F_z=+1} \langle N | \rho_{\mathbf{q}} \rho_{-\mathbf{q}} | N \rangle_{F_z=+1} \\ &= N = \overline{N'}_z, \end{aligned} \quad (74)$$

where $\rho_{\mathbf{q}} \equiv \sum_{\mathbf{k}} a_{1\mathbf{k}-\mathbf{q}}^\dagger a_{1\mathbf{k}}$ is the time independent density operator for $m_F = +1$ particles and $\overline{N'}_z$ is the average number of these particles in this starting state. The correlator is independent of wavevector \mathbf{q} , as well as being time-independent - since we begin in a ground state that

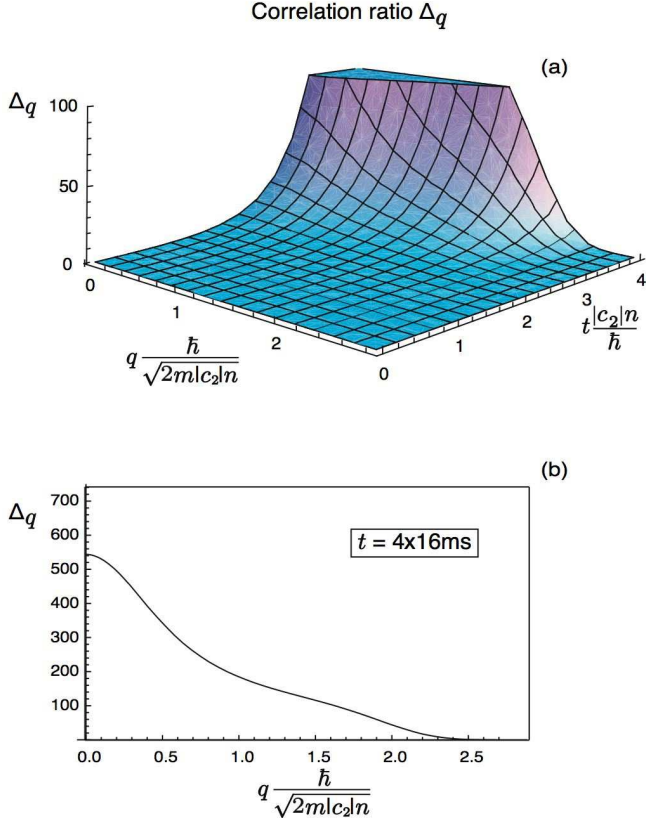


FIG. 9: (Color online) The graphs show the correlation $\Delta_{\mathbf{q}}$ for: (a) a range of times and wavevectors and (b) for a given time of $t = 4 \times 16 \text{ms}$. At this time the signal to Poissonian noise ratio is $\mathcal{O}(10^2)$.

has no dynamics.

(ii) In the second proposed setting, the starting state would be that corresponding to the Berkeley experiments¹, and modeled in this paper, with N particles in the $m_{F_z} = 0$ state. This we predict would exhibit a thermal distribution for the particles in the $m_F = +1$ state, showing super-Poissonian statistics. The density-density correlator for non-zero wavevector \mathbf{q} for this state is time dependent, and we use the time dependent creation operators already derived in this paper:

$$\begin{aligned} C_{0\mathbf{q}} &\equiv {}_{F_z=+1} \langle N | \rho_{\mathbf{q}}(t) \rho_{-\mathbf{q}}(t) | N \rangle_{F_z=+1} \\ &= \sum_{\mathbf{k}} \bar{N}_{1\mathbf{k}} (1 + \bar{N}_{1\mathbf{k}-\mathbf{q}}), \end{aligned} \quad (75)$$

where $\rho_{\mathbf{q}}(t) \equiv \sum_{\mathbf{k}} a_{1\mathbf{k}-\mathbf{q}}^\dagger(t) a_{1\mathbf{k}}(t)$ is the time dependent density operator for $m_{F_z} = +1$ particles, and $\bar{N}_{1\mathbf{k}}$ was defined in Eq.(36). The comparison of the two settings, by looking at the ratio of the experimentally computed correlations for each case and comparing to the theoretical predictions, would provide a direct verification of the unique statistics associated with the two-mode squeezing in these $F = 1$ spinor condensates. We may define a

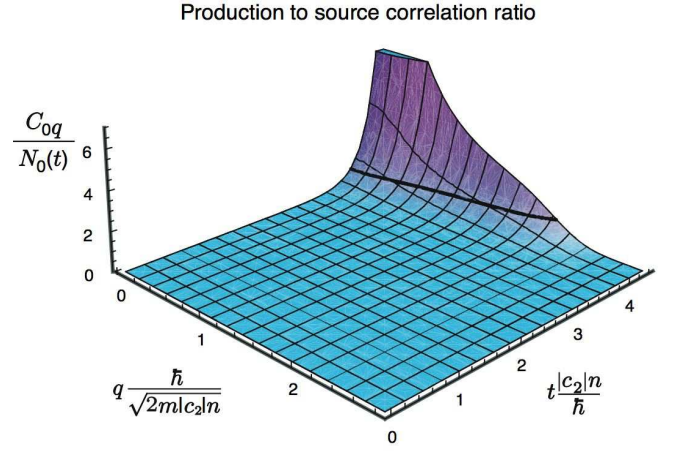


FIG. 10: (Color online) The ratio $C_{0\mathbf{q}}/N_0(t)$ grows above unity, at later times (indicated by the region above the black curve).

correlation ratio deviation, $\Delta_{\mathbf{q}}$, implicitly,

$$\frac{C_{0\mathbf{q}}}{C_{+\mathbf{q}}} = 1 + \Delta_{\mathbf{q}}. \quad (76)$$

The correlation ratio deviation shows us how much the noise differs from that of a coherent state and corresponds to a signal to noise figure for an experiment. For our model we may calculate numerically $\Delta_{\mathbf{q}}$ as a function of time, using for $C_{+\mathbf{q}}$ the number of $m_F = +1$ particles present in our sample at a given time, having been produced from our initial $m_F = 0$ source,

$$\Delta_{\mathbf{q}} = \frac{\sum_{\mathbf{k}} \bar{N}_{1\mathbf{k}} \bar{N}_{1\mathbf{k}-\mathbf{q}}}{\sum_{\mathbf{k}} \bar{N}_{1\mathbf{k}}}. \quad (77)$$

Our calculations, shown in Fig. (9), indicate an expected $\Delta_{\mathbf{q}}$ to be $\mathcal{O}(10^2)$ for initial times $t \sim 4 \times 16 \text{ms}$. This suggests that the thermal noise should be readily observable in a typical experimental setting. Furthermore if we look at the ratio $C_{0\mathbf{q}}/N_0(t)$, Fig.(10), which is the ratio of the density-density correlator for our starting state to the Poissonian density-density correlator expected for the number of $m_F = 0$ source particles remaining in the sample at any given time, $N_0(t)$, we see that, say at times $\sim 4 \times 16 \text{ms}$, this is greater than unity. This suggests that at this time, and onwards, the thermal correlations are greater than the Poissonian system shot noise and should be experimentally observable. Such an experiment to probe the correlations in Bose-Einstein condensed gases has been proposed by Altman et al.⁵⁰ The experimental effect of super-Poissonian statistics is reminiscent of the Hanbury-Twiss-Brown effects⁵¹, and the varying number statistics in our case are due to the perfect correlations between $m_F = \pm 1$ pairs in the Berkeley experiments.

V. SUMMARY

In this paper we have discussed the seeding of domains in the magnetic system of a Bose-Einstein spinor condensate of ^{87}Rb atoms, in the spin triplet $F = 1$. The analysis was performed in the context of the experiment performed by Sadler et al.¹. The spinor gas behaves ferromagnetically, and the experiment showed the emergence of domains of transverse magnetization evolving from an initial polar state in the $m_F = 0$, that becomes dynamically unstable as the initial magnetic field is quickly ramped down.

We have described the dynamical quantum fluctuations of such a sample that starts as a condensate of N atoms in a pure $F = 1$, $m_F = 0$ in analogy to the ‘two-mode squeezing’ of quantum optics. Specifically we have modeled the initial $m_F = 0$ condensate as a source for the creation of particle pairs in the $m_F = \pm 1$ states. Our considerations for the single-mode Hamiltonian were extended to a multi-mode approximation which lead us to a representation of the system via an $\mathfrak{su}(1,1)$ algebra. Even though the system as a whole is described by a pure state with zero entropy, it turned out that considering only one species at a given wavevector at a time we obtain super-Poissonian fluctuations that correspond to a thermal state. This may be thought of as equivalent to considering the reduced density matrix for the $m_F = 1$ degree of freedom, by tracing out the $m_F = \{-1, 0\}$ degrees of freedom. These quantum fluctuations of the initial dynamics of the system provide the seeds for the formation of domains of ferromagnetically aligned spins. The super-Poissonian fluctuations should be observable experimentally by looking at density-density correlations to compare our time-evolved states to coherent states.

We should finally note that if we were to use a mean-field Gross-Pitaevskii approach then we would not observe the evolution of the system in the absence of noise. Our approach provides the source of the instability needed for the Gross-Pitaevskii equation, in terms of the quantum noise of squeezed quantum states. As an improvement on the standard mean field description of the system, one may try to match the fluctuations of the quantum states to the initial boundary conditions for the mean-field Gross-Pitaevskii equations - such an approach has appeared in the work of Saito et al.²². This provides a semi-classical but fully non-linear description that may probe the system in the metastable time regime, after the domain formation is complete, to investigate their stability and evolution. The evolution of the uniform starting state into domains may be viewed a process akin to the Kibble-Zurek mechanism^{21,22,42,43} originally developed to describe the initial evolution of cosmological defects in the early Universe. Furthermore the processes described have analogues in different models for the production and statistics of particles in cosmology^{39,40,52}. It may be possible in the future to even make the connection more explicit and perhaps even get to the point of using Bose-Einstein spinor condensates as analogue models for cosmological considerations^{53,54,55}.

Acknowledgments

We are grateful for helpful conversations with M. Baraban, F. Song and L. Glazman. GIM and SMG were supported by NSF DMR-0603369 and NRC was supported by EPSRC grant GR/S61263/01.

* Electronic address: george.mias@aya.yale.edu

† Electronic address: nrc25@cam.ac.uk

‡ Electronic address: steven.girvin@yale.edu

¹ L. E. Sadler, J. M. Higbie, S. R. Leslie, M. Vengalattore, and D. M. Stamper-Kurn, *Nature* **443**, 312 (2006).

² D. M. Stamper-Kurn, M. R. Andrews, A. P. Chikkatur, S. Inouye, H.-J. Miesner, J. Stenger, and W. Ketterle, *Phys. Rev. Lett.* **80**, 2027 (1998).

³ J. Stenger, S. Inouye, D. M. Stamper-Kurn, H. J. Miesner, A. P. Chikkatur, and W. Ketterle, *Nature* **396**, 345 (1998).

⁴ T. L. Ho, *Phys. Rev. Lett.* **81**, 742 (1998).

⁵ M. Koashi and M. Ueda, *Phys. Rev. Lett.* **84**, 1066 (2000).

⁶ T. Ohmi and K. Machida, *J. Phys. Soc. Jpn* **67**, 1822 (1998).

⁷ C.-C. Chang, N. Regnault, T. Jolicoeur, and J. K. Jain, *Phys. Rev. A* **72**, 013611 (2005).

⁸ M. S. Chang, C. D. Hamley, M. D. Barrett, J. A. Sauer, K. M. Fortier, W. Zhang, L. You, and M. S. Chapman, *Phys. Rev. Lett.* **92**, 140403 (2004).

⁹ M.-S. Chang, Q. Qin, W. Zhang, L. You, and M. S. Chapman, *Nat Phys* **1**, 111 (2005).

¹⁰ H.-J. Miesner, D. M. Stamper-Kurn, J. Stenger, S. Inouye,

A. P. Chikkatur, and W. Ketterle, *Phys. Rev. Lett.* **82**, 2228 (1999).

¹¹ D. M. Stamper-Kurn, H.-J. Miesner, A. P. Chikkatur, S. Inouye, J. Stenger, and W. Ketterle, *Phys. Rev. Lett.* **83**, 661 (1999).

¹² A. Lamacraft, *Physical Review Letters* **98**, 160404 (2007).

¹³ C. K. Law, H. Pu, and N. P. Bigelow, *Phys. Rev. Lett.* **81**, 5257 (1998).

¹⁴ H. Pu, C. K. Law, S. Raghavan, J. H. Eberly, and N. P. Bigelow, *Phys. Rev. A* **60**, 1463 (1999).

¹⁵ S. Yi, O. E. Mustecaplioglu, and L. You, *Phys. Rev. A* **68**, 013613 (2003).

¹⁶ T. Isoshima, K. Machida, and T. Ohmi, *J. Phys. Soc. Jpn* **70**, 1604 (2001).

¹⁷ H. Saito, Y. Kawaguchi, and M. Ueda, *Phys. Rev. Lett.* **96**, 065302 (2006).

¹⁸ H. Saito, Y. Kawaguchi, and M. Ueda, *Phys. Rev. A* **75**, 013621 (2007).

¹⁹ H. Saito and M. Ueda, *Phys. Rev. A* **72**, 023610 (2005).

²⁰ Y. Kawaguchi, H. Saito, and M. Ueda, *Phys. Rev. Lett.* **98**, 110406 (2007).

²¹ B. Damski and W. H. Zurek, *Phys. Rev. Lett.* **99**, 130402

- (2007).
- ²² H. Saito, Y. Kawaguchi, and M. Ueda, Phys. Rev. A **76**, 043613 (2007).
- ²³ G. I. Mias, Ph.D. thesis, Yale University (2007).
- ²⁴ F. Dalfovo, S. Giorgini, L. P. Pitaevskii, and S. Stringari, Rev. Mod. Phys. **71**, 463 (1999).
- ²⁵ B. D. Esry and C. H. Greene, Phys. Rev. A **60**, 1451 (1999).
- ²⁶ A. J. Leggett, Rev. Mod. Phys. **73**, 307 (2001).
- ²⁷ C. Pethick and H. Smith, *Bose-Einstein condensation in dilute gases* (Cambridge University Press, Cambridge, 2002).
- ²⁸ E. M. Lifshitz and L. D. Landau, *Mechanics* (Butterworth-Heinemann, 1982).
- ²⁹ R. B. Diener and T.-L. Ho, cond-mat/0608732 (2006).
- ³⁰ N. P. Robins, W. Zhang, E. A. Ostrovskaya, and Y. S. Kivshar, Phys. Rev. A **64**, 021601(R) (2001).
- ³¹ W. Zhang, D. L. Zhou, M. S. Chang, M. S. Chapman and L. You Phys. Rev. Lett. **95**, 180403 (2005).
- ³² E. M. Lifshitz and L. D. Landau, *Statistical physics* (Butterworth-Heinemann, 1984).
- ³³ D. F. Walls, Nature **306**, 141 (1983).
- ³⁴ D. Walls and G. Milburn, *Quantum optics* (Springer, Berlin, 1995).
- ³⁵ R. R. Puri, *Mathematical methods of quantum optics* (Springer, Berlin, 2001).
- ³⁶ C. M. Caves and B. L. Schumaker, Phys. Rev. A **31**, 3068 (1985).
- ³⁷ A. T. Black, E. Gomez, L. D. Turner, S. Jung, and P. D. Lett, cond-mat/arxiv.org:0704.0925 (2007).
- ³⁸ C. Gardiner and P. Zoller, *Quantum noise : a handbook of Markovian and non-Markovian quantum stochastic methods with applications to quantum optics* (Springer, Berlin, 2000).
- ³⁹ A. H. Guth and S.-Y. Pi, Phys. Rev. D **32**, 1899 (1985).
- ⁴⁰ A. Hamilton, D. Kabat, and M. Parikh, Journal of High Energy Physics **2004**, 024 (2004).
- ⁴¹ S. W. Hawking, Communications in Mathematical Physics **43**, 199 (1975).
- ⁴² T. W. B. Kibble, Journal of Physics A **9**, 1387 (1976).
- ⁴³ W. H. Zurek, Nature **317**, 505 (1985).
- ⁴⁴ B. C. Hall, *Lie groups, Lie algebras, and representations : an elementary introduction* (Springer, New York, 2003).
- ⁴⁵ A. W. Knap, *Lie groups beyond an introduction* (Birkhäuser, Boston, 2002).
- ⁴⁶ C. C. Gerry, Phys. Rev. A **31**, 2721 (1985).
- ⁴⁷ W. E. Boyce and R. C. DiPrima, *Elementary differential equations and boundary value problems* (Wiley, Hoboken, NJ, 2005).
- ⁴⁸ P. Drummond, Z. Ficek, and eds, *Quantum squeezing* (Springer, Berlin, 2004).
- ⁴⁹ R. J. Glauber, Phys. Rev. **130**, 2529 (1963).
- ⁵⁰ E. Altman, E. Demler, and M. D. Lukin, Phys. Rev. A **70**, 013603 (2004).
- ⁵¹ R. H. Brown and R. Q. Twiss, Nature **177**, 27 (1956).
- ⁵² S. W. Hawking, Phys. Rev. Lett. **26**, 1344 (1971).
- ⁵³ G. E. Volovik, Physics Reports **351**, 195 (2001).
- ⁵⁴ G. E. Volovik, Journal of Low Temperature Physics **124**, 25 (2001).
- ⁵⁵ G. E. Volovik, *The universe in a helium droplet* (Oxford University Press, USA, 2003).